Computer Simulation of the Periodic Electrostatic Focusing Converter

By William L. Barr, Barry C. Howard, and Ralph W. Moir;
Lawrence Livermore Laboratory; University of California, Livermore, CA 94550

Contact information as of 2009 for Ralph Moir is Vallecitos Molten Salt Research, <RMoir@Pacbell.net>, 607 East Vallecitos Road, Livermore, CA 94550.

Abstract

A computer study was made of the various physical processes that take place in the periodic electrostatic focusing, direct energy converter. Computer simulation techniques are described and the results are presented. The effect that space charge, secondary electrons, beam size, charge exchange, and ionization have on conversion efficiency is examined. The results are applied to the design of a reactor. Finally, future plans for studies of direct converters are discussed.

Introduction

The periodic electrostatic scheme[1] for direct energy recovery is being studied using computer simulation techniques[2]; Specifically, the computer code DART[3] has been developed to calculate the efficiency of energy recovery by following several hundred ion trajectories through a magnetic expander and a direct converter.

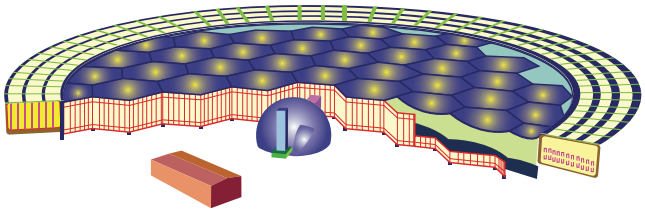

Figure 1 — A mirror-type reactor surrounded by the magnetic expander and direct recovery system.

Figure 1 is an artist's conception of a reactor showing a fan-shaped magnetic expander and a direct recovery system around the outside circumference[4]. The ion trajectories have been followed:

- Down the magnetic expander
- Through the diverter-separator
- Through the electrostatic electron repeller
- Down the channel where electrostatic focusing and self-consistent space-charge fields are calculated
- Out until collected at some electrode

Secondary electrons are started with an energy-dependent emission coefficient at every point where an ion trajectory intercepts any grid or solid electrode.

Flexibility in DART stems from solving Poisson's equation for potential by using an over-relaxation numerical technique that allows for unusually shaped boundaries. In this way, only the boundary values of potential need to be given. The steady state charge density is obtained from the trajectories by iteration. Figure 2 shows some typical trajectories leaving the expander and proceeding on to collection.

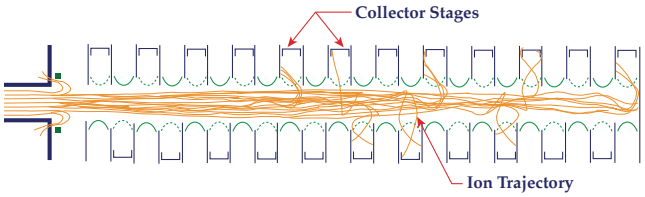

Figure 2 — Ion trajectories inside the focusing and collecting system.

In the absence of space charge, the potential in the channel region is given by

$$V = V_0\left[\frac{x}{L} + \left(\frac{c}{2\pi}\right)\sin\left(\frac{2\pi x}{L}\right)\sinh\left(\frac{2\pi z}{L}\right)\right] \quad (1)$$

where L is the spatial period, V_o is the amount by which the potential on the axis increases in distance L, and C is the focus-strength parameter.

Initial Conditions

To optimize design parameters and to study space charge, ion trajectories were started just before the diverter separator at the exit end of the expander. Deuterons were started with 40 different energies equally spaced from 400 to 1200 keV.

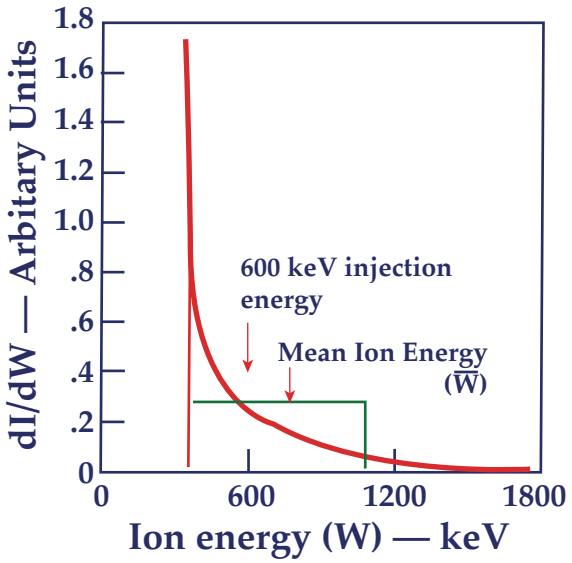

Figure 3 — The expected energy distribution[5] compared to the flat-topped distribution used in the report.

Figure 3 compares this flat-topped distribution with the expected distribution as calculated by a Fokker-Planch code.[5] At each energy, nine different trajectories were run with different initial distances from beam center and with appropriate directions for the velocity vectors.

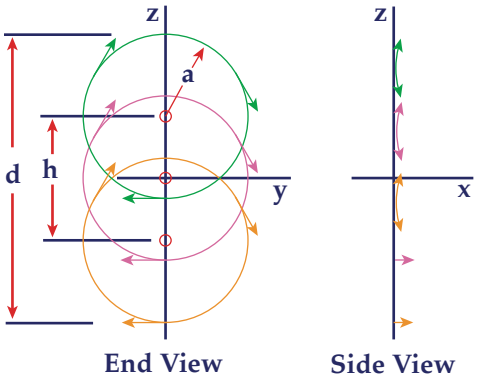

Figure 4 — Nine trajectories used at each energy to define the incident beam at the magnetic mirror. Larmoir radius (a) depends on energy.

Figure 4 shows the nine trajectories. A total of 360 trajectories were used to represent a flat-topped energy distribution with a 3-to-1 energy spread. Beam thickness (d) is determined by the radius (a) of the orbits inside the expander plus the thickness (h) of the flux tube that links the expander to the reactor:

$$d = h + 2a$$

Space-Charge Effects

Figure 5 shows a plot of η, the calculated efficiency of energy recovery, vs p/l, the total power input per unit length of circumference. The error bars on the calculated points indicate than ±1% uncertainty resulting from the finite number of trajectories. Each point represents the highest efficiency obtained at that power level as the width of the channel and the strength of the focusing electric field were changed. The straight line through the points is not only the best fit to the points, but is also the curve predicted theoretically by Marcus.[6]

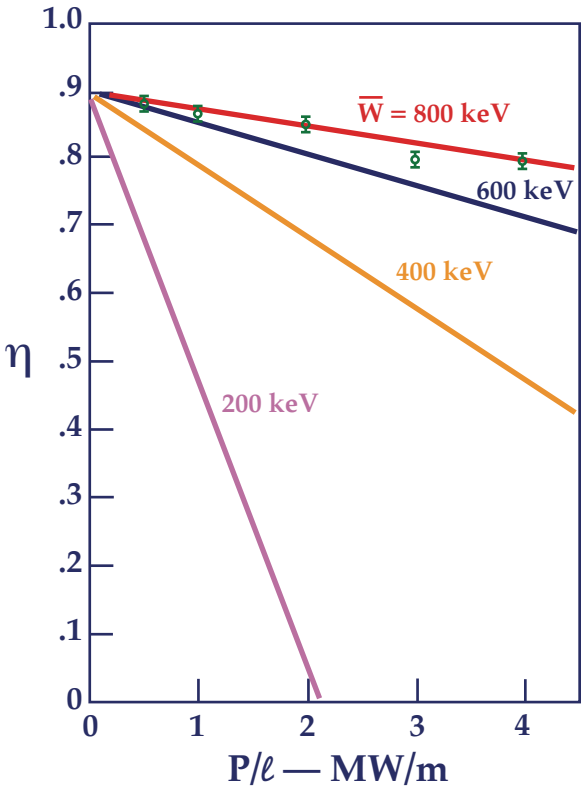

Figure 5 — Collection efficiency versus power level for several different mean energies.

We used the theory developed by Marcus to draw the curves for other mean energies shown in the figure. In drawing the curves we assumed that all dimensions of the device were scaled in proportion for the beam $W^{1/2}$, where W is the average ion energy. The dependence of efficiency on d, W, and p/ℓ can be obtained from Marcus's results. He found

$$\eta = \eta_0 - 2.6\left(\omega_p \tau\right)^2 \left(\frac{d}{L}\right)^2 \quad (2)$$

where η_0 is the efficiency at zero density. When $(\omega_p\tau)^2$ is expressed in terms of p/ℓ and W the efficiency becomes

$$\eta = \eta_0 - 2.6\left(\frac{q^2}{2\varepsilon_0}\right)\sqrt{\frac{M}{2}}\left(\frac{d}{\overline{W}^{5/2}}\right)\left(\frac{p}{\ell}\right) \quad (3)$$

If we substitute the numerical values appropriate to D+ ions, and use $\eta_0 = 0.90$ obtained from the data shown in Figure 5, we get:

$$\eta = 0.90 - 0.026\left(\frac{p}{\ell}\right)d\left(\frac{800}{\overline{W}}\right)^{5/2} \quad (4)$$

where p/ℓ is in MW/m, d is in m, and $\overline{W}$ is in keV.

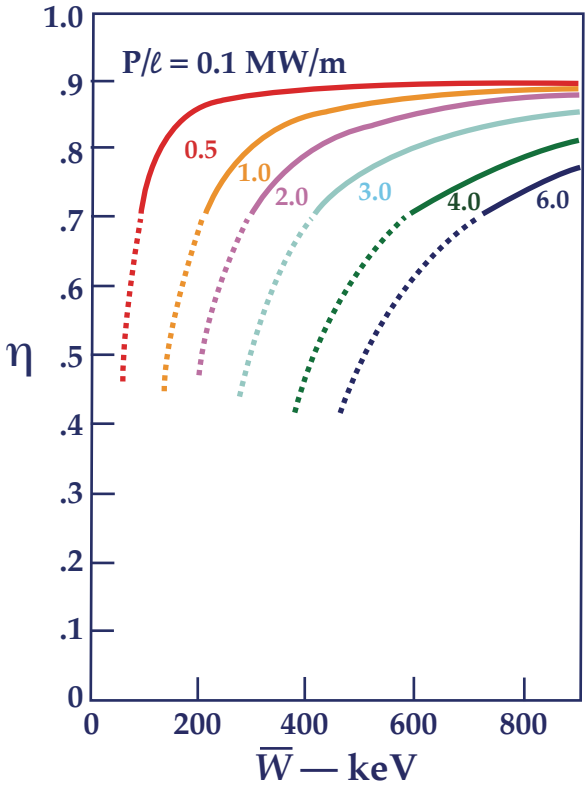

Figure 6 — Collection efficiency vs mean energy for different power levels.

The same equation is plotted differently in Figure 6. Here η is plotted against $\overline{W}$ with p/ℓ as a parameter. Again, d was assumed proportional to $\sqrt{\overline{W}}$. As a comparison, in a recent engineering study[7] of a different reactor design, it was assumed that $\overline{W}$ = 620 keV, p/ℓ = 3 MW/m, and that the overall efficiency of the direct converter was 70%. It can been seen in Figure 5 that this allows about 5% for other losses not included in the figure.

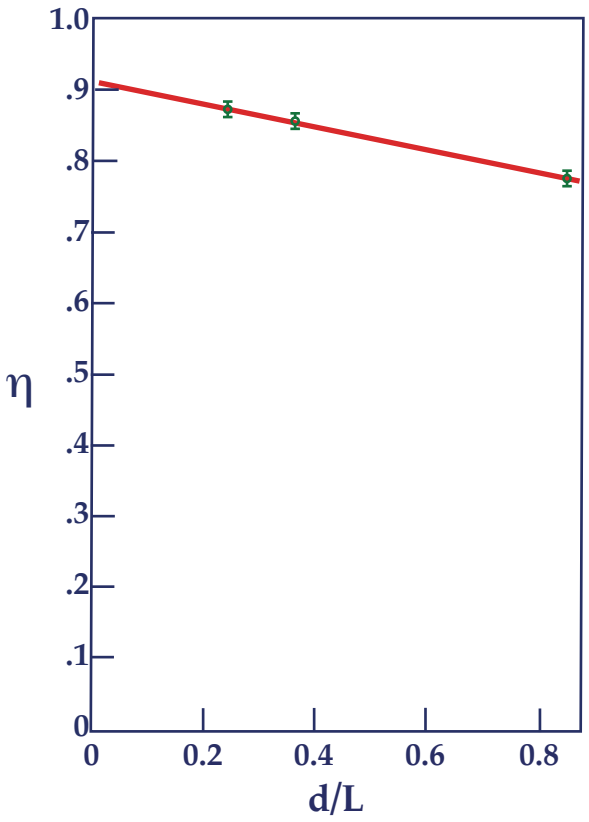

Figure 7 — Collection efficiency vs beam thickness (d). Here p/ℓ = 2 MW/m, $\overline{W}$ = 800 keV, and L = 2m.

Figure 7 shows η plotted against d for the case where p/ℓ = 2 MW/m and $\overline{W}$ = 800 keV. The points were calculated by computer and the solid curve is from Equation 4. Any lack of agreement might be due to the change in the structure of the beam as d is varied. This change in structure results because only the flux tube is changed, not the orbit sizes or pitch angles inside the expander.

Insight into the nature of the space-charge effects in the periodic focusing system can be obtained from studying Figure 8. This figure shows the efficiency, averaged over a flat-topped three-to-one energy distribution, plotted against the difference in potential ΔV between a pair of focus electrodes opposing each other across the channel.

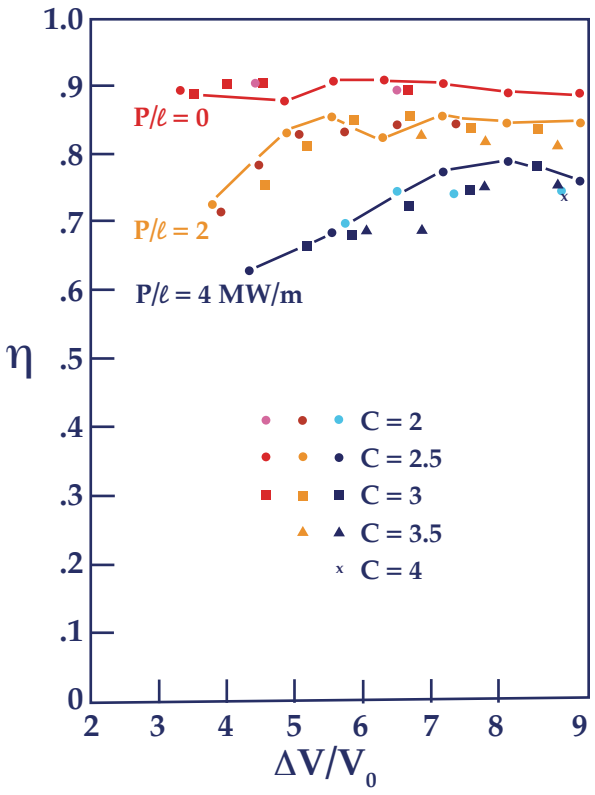

Figure 8 — Collection efficiency versus potential difference between an opposing pair of focus electrodes across the channel from each other.

For a given power level, the points fall fairly well along a smooth curve regardless of what combination of channel width and focusing field results in each value of ΔV. Focusing field strength is proportional to the constant C indicated on the figure. The curves have a knee below which the efficiency falls off rapidly with decreasing ΔV. Above the knee there is a little change inefficiency with increased ΔV. The knee occurs at higher ΔV the higher the power level. (It is important to keep ΔV as small as possible for voltage holding considerations).

We can explain the shift in efficiency by considering the model used by Marcus. In that model, the ions at the boundaries of the beam oscillate back and forth between the space charge of the beam and the effective average focusing potential of the electrodes. The effective potential, determined by ΔV, must be at least as high as the space charge potential of the beam to confine the ions and prevent their premature loss from the beam.

Secondary Electron Effects

To determine the loss efficiency due to secondary electrons, the DART computer code was expanded to start and follow electron trajectories from each point on any grid or solid surface (except the end wall and the negative stage) that is intercepted by an ion trajectory. The number of electrons released per ion is ϒ on a solid surface and (1-T)ϒon a grid of transmissivity equal to T. The value of the emission coefficient ϒ is determined by the velocity of the ion at the time of impact. The formula used for ϒ is:

$$\begin{aligned} \gamma &= 0.1; && W \le 2.0 keV \\ \gamma &= 0.1 + 0.3841 nW/2; && 2 < W < 280 \quad (5) \\ \gamma &= 2; && W \ge 280 \end{aligned}$$

where W is the energy of the D+ ion in keV at the point of impact. This formula gives a good fit to the published data for D+ impacting on Mo[8] and for H+ impacting on Mo[9] and W[10] when compared at equal velocities (see Figure 9).

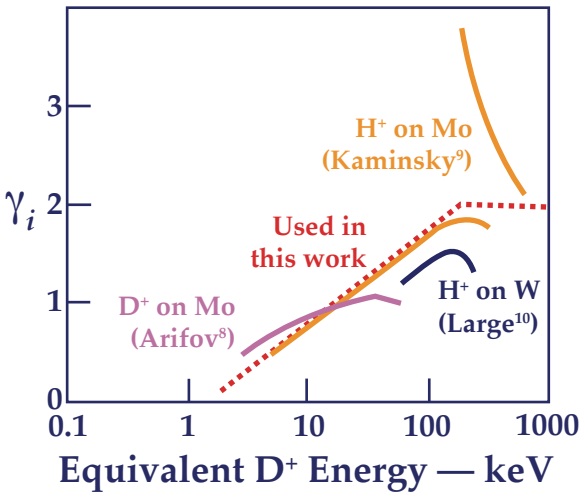

Figure 9 — Secondary electron emission coefficient vs ion energy.

A fraction, 1-T, of the ion current is assumed to be collected on a grid at each passage through a grid. Then only T^n of the current represented by an ion trajectory remains after n passes through the grids. The electrons are released with 0.1 keV of energy and with their velocity vectors directed opposite to that of the ion at impact. We ignored the effect of the incidence angle on ϒ at the grid wires. The effect of angle is expected to multiple ϒ by the secant of the angle to the normal, so that the average effect should be to increase ϒ by π/2 on wires.

Since the number of electrons born on grids in proportional to 1-T, and the number born on solid surfaces is proportional to T, it is easy to compare the relative losses by varying T. We. made three runs where the parameters were identical except for T (the space charge was zero). The loss of efficiency due to secondaries in the different runs was:

T	Δη
0.97	-0.0577
0.98	-0.0430
0.985	-0.0355

These values fit the relation:

$$\Delta\eta = -1.493(1-T) - 0.0133T \quad (6)$$

Therefore, an ion striking a grid produces electrons that carry away 1.493/0.013 = 112 times as much energy, on the average, as the electrons produced when an ion strikes a collector surface. This is because electrons produced on collectors usually fall back onto the collector while electrons produced on grids always leave and usually fall onto the most positive neighboring electrode.

Surface-charge effects and secondary electron effects are nearly independent of each other because the potential is only slightly modified by space charge. What little combined effect there is results from the modified ion trajectories with space charge. Ion collection efficiency is not as good then, and more ions strike outer electrodes from which the electrons can escape. This effect was minimized by shortening all fins equal to the shortest of the two that were used until now.

The scaling of the loss in efficiency with ion energy can be obtained from Equation 6 by noting that $1-T \propto r/l$, where r is the radius of a grid wire. The minimum value for r is determined by breakdown potential and electrical field at the wire. This gives[11] $r \propto V_o$, and for a given number of stages $V_o \propto W$. Therefore, since $L \propto d \propto W^{1/2}$, as discussed earlier, we see that $\Delta\eta \propto W^{1/2}$ is proportional to $W^{1/2}$.

To evaluate the actual loss due to secondaries we need to know how small r (and hence $1-T$) can be made before sparking occurs. We can calculate the electric field at the wire in a geometry that is roughly correct where the electric field is strongest. This happens where the grid faces a neighboring fin (see Figure 2).

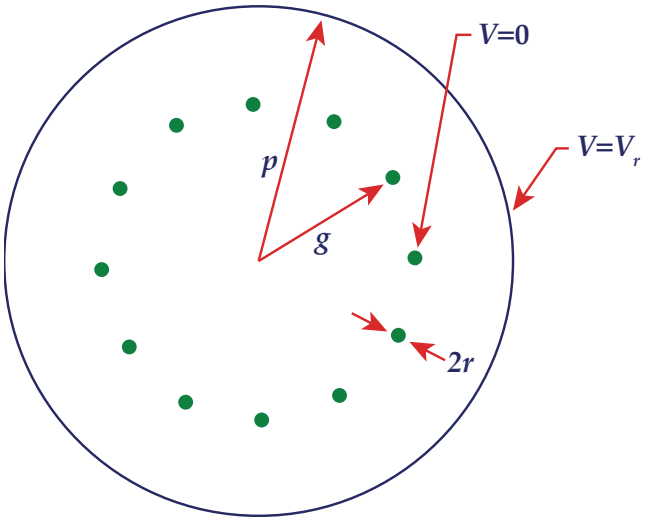

Figure 10 — Simplified geometry for calculating the electric field at the grid wires.

In the cylindrical geometry of Figure 10, with N equally spaced grid wires and no center electrode, the strongest electric field is at the outer face of a grid wire. There, the electric field E is:

$$E = \left(\frac{V_p}{r}\right)\ln\left[\frac{g}{Nr}\left(\frac{p}{g}\right)^N\right] \quad (7)$$

where V_p is the difference in potential between fin and grid, as determined from Eq. 1. Here, C = 2.5, L = 2 m, V_o = 100 kV when W = 800 keV, and Z = 0.84 m at a grid. Thus, V = 3 x 10^5 V. The other parameters are $p = L/4$ = 0.5 m, N = 20, $r = (1-T)L/2N$, $g = ap$. Then, in terms of a and T, E becomes

$$\left(6x10^4 V/cm\right)\left((1-T)\ln\left[2(1-T)a^{21}\right]\right) - 1 \quad (8)$$

The plate-to-grid spacing is $p-g = (1-a)p$. Equation 8 is shown plotted in Figure 11.

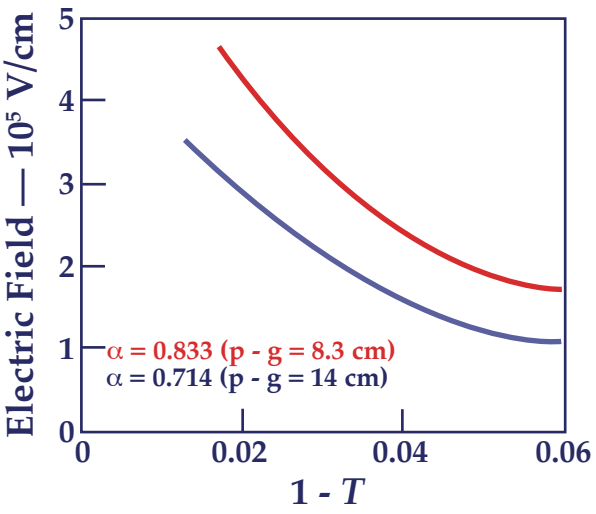

Figure 11 — Electric field at a grid wire vs the optical opacity of the grid. (See Figure 10 for p-g.)

In an earlier engineering study[4] it was decided that E = 1 x 10^5 V /cm is a "modest gradient for vacuum insulation." We assume here that 3 x 10^5 V /cm is possible. Then, 1-T = 0.03 and the loss due to secondary electrons in only about 6% when $\overline{W}$ = 800 keV. The above scaling law then predicts a 3% loss at 200 keV, 4% at 350 keV and 5% at 550 keV.

Charge Exchange and Ionization Losses

Of the remaining loss mechanisms, charge exchange on background gas is the most important at low energy. If an ion exchanges charge states with a neutral molecule, its energy becomes inaccessible for direct recovery and so must be counted as a loss to the direct converter. The energy may still be recovered in a thermal cycle, but at lower efficiency. If the collision occurs inside the direct converter, not only is the energy of the primary ion lost, but also energy is lost in accelerating the cold ion.

First, consider the loss due to charge exchange in the expander. The probability that an ion with energy W will undergo charge exchange in going a distance ℓ is

$$P = 1 - e^{-n\sigma\ell} \quad (9)$$

where n is the density of neutral molecules and σ = σ(W) is the cross-section. The probable loss of energy per ion is $\Delta W = WP$ so that the fractional energy loss from the beam is:

$$\Delta\eta = \frac{\int_0^{\infty} WP \frac{dI}{dW} dW}{\int_0^{W} \frac{dI}{dW} dW} \quad (10)$$

However, $P = n\sigma\ell$ whenever $n\sigma\ell << 1$.

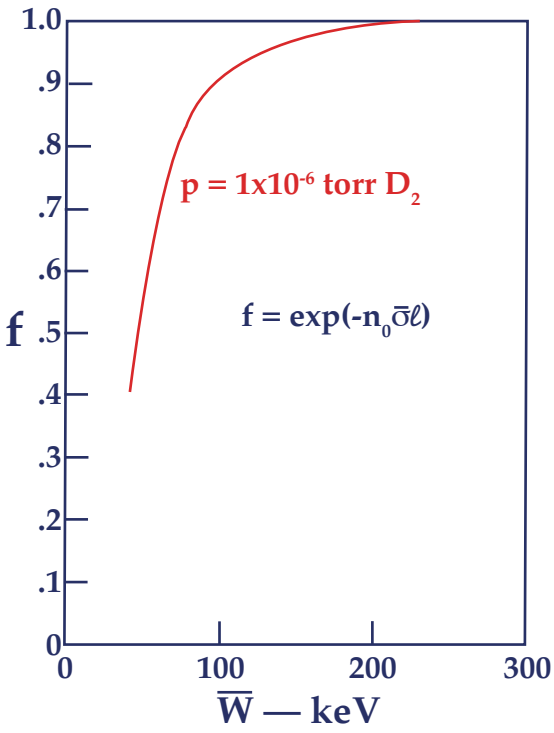

Figure 12 — The fraction of the D+ ions that do not charge exchange vs mean ion energy. Pumping speed and beam power are held constant.

Figure 12 shows a plot of f = 1 - Δη calculated in this way. The following assumptions have been made:

- ℓ = 100 m
- dI/dW is taken from the loss cone distribution calculated by Artcher H. Futch[5] for 100-keV injections, and was simply scaled to other energies.
- Total ion current (and hence has throughput) varies inversely with mean energy because the power is held constant.
- Vacuum pumping speed is constant, with the result that pressure varies directly with gas throughput. The curve was normalized for a pressure of 1 x 10^{-6} torr at a mean energy of 150 keV.
- σ(W) = σ_{10} for D^+ in D_2

The loss is seen to be negligible for mean energy above 300 keV, but becomes forbidding for energies much below 100 keV.

There will also be ionizing collisions between incident ions and gas molecules. When these take place in the expander, the effect is negligible. Only a few percent of the ions suffer these collisions, and when they do they only lose a small fraction of their energy. The resulting cold ions and electrons will follow the magnetic field lines into the diverter at the end of the expander.

When either charge exchange or ionization occurs inside the periodic focusing channel, the results can be more serious. The resulting cold ion and electron will be accelerated in different directions and finally collected on different electrodes. This produces a drain on the power supply that maintains the voltages,and hence lowers the efficiency.

The losses due to charge exchange and ionization inside the direct converter were studied with the computer code DART. Cold ions and cold electrons were started at uniformly distributed points in the region occupied by the ion beam.[12] Briefly, the loss results from the cold ions falling into the potential wells at the grids and eventually being collected on grid wires. Secondary electrons produced at the wires are then accelerated away and account for most of the loss. If p = 1 x 10^{-5} torr D_2 in the direct converter, and if Υ = 2 is the secondary electron coefficient, the loss is 3.3% and 2.87T for c-values of 3.0 and 2.5 respectively. This and voltage-holding considerations, suggest an operating pressure of about 5 x 10^{-6} torr where the loss is about 1.5%.

Other Losses

The loss mechanisms discussed above all depend on particle trajectories and are included in the computer calculations. In addition, there are losses involved in:

1) Coupling the expander to the reactor.
2) Intercepting ions by support columns in the expander.
3) Using power to maintain the vacuum in the expander and converter.
4) Using the inverter-rectifier system to reduce the electrical power output to a common voltage.

The loss due to each of these mechanisms will depend on the actual design.

Item 1 was studied by Gustav Carlson[13] who found that local weakening of one of the magnetic mirrors in the reactor at the entrance to the expander results in less than 95% of the leadage ions finding the direct converter (95% when the mirror ratio R=3 and $\Delta R/R$ = 10%). However, if electrostatic stoppering[14] can be used the coupling can probably be nearly 100% efficient. Figure 13 indicates how electrostatic stoppering might be used to make the leakage more selective. We assume somewhat arbitrarily, a loss of 2% (this was also assumed in Reference 12).

Richard W. Werner, et al.[15] studied item 2 and concluded that support columns would intercept 2% of the ion passing down the expander.

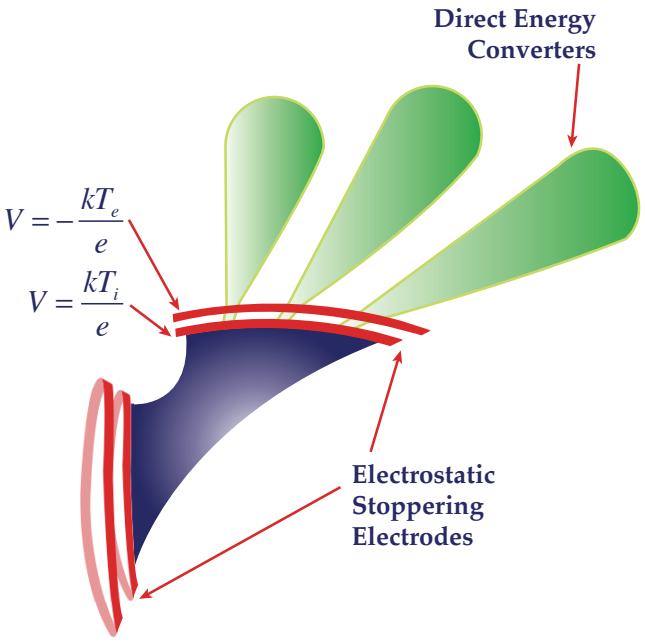

Figure 13 — Venetian Blind direct energy converter. The figure shows how electrostatic stoppering might be used to make the leakage of plasma from the mirror reactor more selective.

The power used by the vacuum pumps (item 3) is small because the gas throughput is small at the high energy where periodic focusing is useful (see Figure 6). Also, the vacuum requirement is modest; p = 1 x 10^{-5} torr is required for voltage-holding and for control of gas ionization in the converter. At 600 keV mean energy, the gas throughput is 2.8 x 10^4 liters/s per MW at 5 x 10^{-6} torr. Large oil diffusion pumps consume about 28 kW of power to pump 2.8 x 10^4 liters/s (i.e., 3.5 x 10^4 liters/s and 36 KW per 1.3 m pump, after allowing for conductance to the pump). Therefore, the pumps would use about 2.8% of the power handled or about 4% of the electrical power output. It seems possible that waste heat could be used for the pumps, in which case the loss due to pumping would be reduced almost to zero.

Item 4 — loss in the inverter-rectifier system — is well documented[2] and should be about 2% of the power handled by the converter. Most of this loss occurs in the power transformers and surge networks used to protect the system against transients.

The total loss due to items 1, 2, and 4 is 6%. This loss, plus the 1.5% loss due to ionization and charge exchange, and the energy-dependent loss due to secondary electrons (3 to 6%) must be subtracted from the efficiency shown in Figure 5 to give the working efficiency of the direct converter. Since the direct converter is followed by a thermal converter, even an inefficient direct converter produces a considerable net gain over thermal conversion alone.

Application to Reactor Design

When all the various losses discussed the last few sections are subtracted from the efficiencies. shown in Figure 6, the result in η_{DC}, the working efficiency of the direct converter. η_{DC} is plotted vs the average ion energy in the upper part of Figure 14 for several different power levels.

Power levels are given in units of MW/m of circumference of the converter (see Figure 1). The required circumference (and therefore size and cost) of the expander and converter is determined by the ratio of total power handled to the power per unit length. At low power levels where the shape of the curves is not dominated by space-charge effects, η_{DC} decreases at high energy because of secondary electron effects. Two curves in Figure 14 show where a four-stage venetian blind converter[16] would be on the plots.

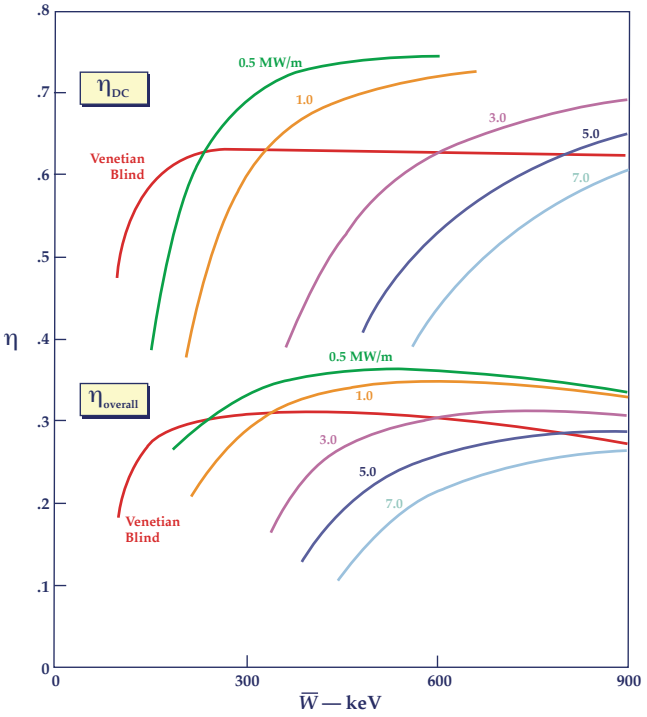

Figure 14 — Working efficiency (η_{DC}) of the direct converter, and overall plant efficiency ($\eta_{overall}$) versus mean energy. The curves labeled Venetian Blind refer to a direct converter.

The lower set of curves in Figure 14 shows the overall efficiency of a mirror reactor equipped with the direct converter described above. The overall efficiency, $\eta_{overall}$ is defined as the ratio of the output electric power to the power produced by the thermonuclear reactions inside the reactor. That is, $\eta_{overall} = P_{out}/(P_{in} \times Q)$,where P_{in} is the injected beam power and Q is the figure of meter defined as the ratio of thermonuclear power to injected power. Values of Q for D-T reactions at the different mean energies were taken from A. H. Futch et al.[17] We increased the valued 30% to allow for the enhancement predicted for a narrow source angle perpendicular to the magnetic field. The fraction, f = 0.157, is the ratio of the thermonuclear power produced in the form of charged particle energy (3.51 MeV) to the total reaction energy (22.4 MeV). The latter energy includes 4.8 MeV released in the lithium blanket when tritium is regenerated.

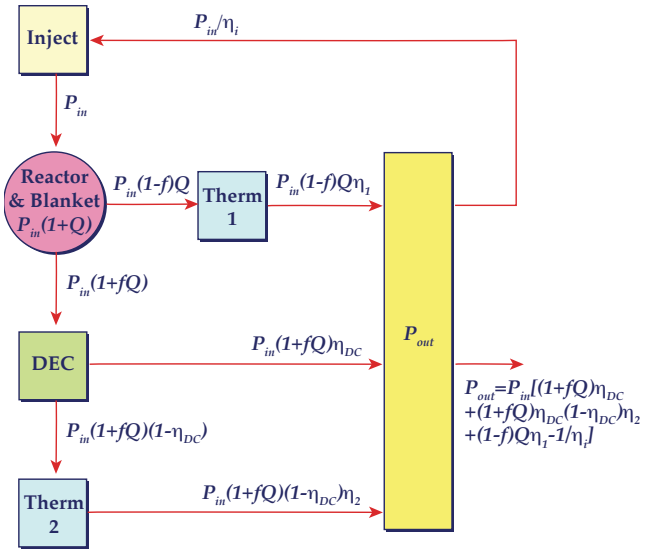

Figure 15 — Power flow diagram for a mirror reactor with a direct converter.

Figure 15 shows a power flow diagram. Two thermal conversion cycles are assumed: Therm. 1, with an efficiency η_1 = 0.45, receives a 1-f fraction of uncharged particle power; Therm. 2, with η_2 = 0.40, forms a bottoming cycle to recover heat from the direct converter. The efficiency (η_I) of the injector for accelerated D-neutralized in a plasma was taken from Hoving hand Moir.[18] Note that the overall efficiency in Figure 15 is given by:

$$\eta_{overall} = \left(\frac{1}{Q} + f\right)\left[\eta_2 + (1-\eta_2)\eta_{DC}\right] + (1-f)\eta_1 - \frac{1}{Q\eta_1} \quad (11)$$

The value $\eta_{overall}$ is also plotted in Figure 14 for the several different η_{DC} shown in the same figure. Table 1 lists the Q-values and efficiencies used. Note that $\eta_{overall}$ has a maximum at an intermediate energy and falls off at a low energy because η_{DC} decreases. At high energy, $\eta_{overall}$ falls off because Q decreases.

The best mean energy for operating the reactor depends on the power level. For example, if 100-MW is handled by the direct converter at 1 MW/m, the circumferential length of the direct converter must be 1000 meters.

Figure 14 — Working efficiency (l1DcJ of the direct converter, and overall plant efficiency (l1 overall) vs mean energy. The curves labeled Venetian Blind refer to a direct converter.

Unless the expander fan can somehow be spread open more than 360°, a diameter of at least 320 m is required. (Incidentally, only about 12 m of radius is required for expanding the beam adiabatically in the magnetic field from 150 kg down to 500 g.)[19] At 3 MW/m the diameter can be reduced to 100 m and the floor area of the evacuated expander can be reduced by -nearly an order of magnitude.

Cost

We estimate that a direct converter with a power density of 3 MW/m will cost $176,000,000 for 1000 MW into the converter. If we required less power density or more power we could obtain it by increasing the circumference. This can be done in two ways: by increasing the radius or by adding more direct converter units. In the first case, the cost would scale as the radius squared. In the second case, the cost would scale linearly with power and inversely with power density.

The latter case seems more reasonable, but it depends on subdividing the leaking plasma, as shown in Figure 13. Adopting the second case and taking the $176 per kW handled (into the converter) we have computed the cost of the direct converter, based on net power, using the efficiencies given in Table 1 and Figure 14. For comparison, the cost bases for the Venetian Blind direct converter was $109 per kW handled.[16]

Table 1 — Parameters Used to Construct Figure 14

W	Q	η_i	η_{DC}					
			0.5 MW/m	1 MW/m	3 MW/m	5 MW/m	7 MW/m	Venetian Blind
100	1.69	0.83	—	—	—	—	—	0.49
125	1.82	0.84	0.184	—	—	—	—	0.56
150	1.82	0.86	0.382	0.003	—	—	—	0.59
200	1.82	0.88	0.565	0.355	—	—	—	0.62
300	1.76	0.89	0.693	0.598	0.218	—	—	0.63
400	1.69	0.91	0.730	0.675	0.463	0.249	0.035	0.63
500	1.63	0.92	0.744	0.708	0.573	0.436	0.300	0.63
600	1.56	0.92	0.748	0.725	0.631	0.536	0.441	0.63
700	1.5	0.92	0.752	0.735	0.664	0.595	0.525	0.63
800	1.43	0.92	0.752	0.739	0.685	0.632	0.578	0.63
900	1.37	0.92	0.750	0.741	0.698	0.656	0.613	0.63

To put these costs in perspective, in 1970 Myers[20] estimated that, to be economically competitive, the cost for the nuclear part of the power plant (magnetic, blanket, injector and direct converter) should range from $80 to $103 per kW, of less. Much has happened in the energy field in the last four years and Myers[21] now estimates that by 1980 these costs will range from $180 to $290 per kW (1974 dollars).

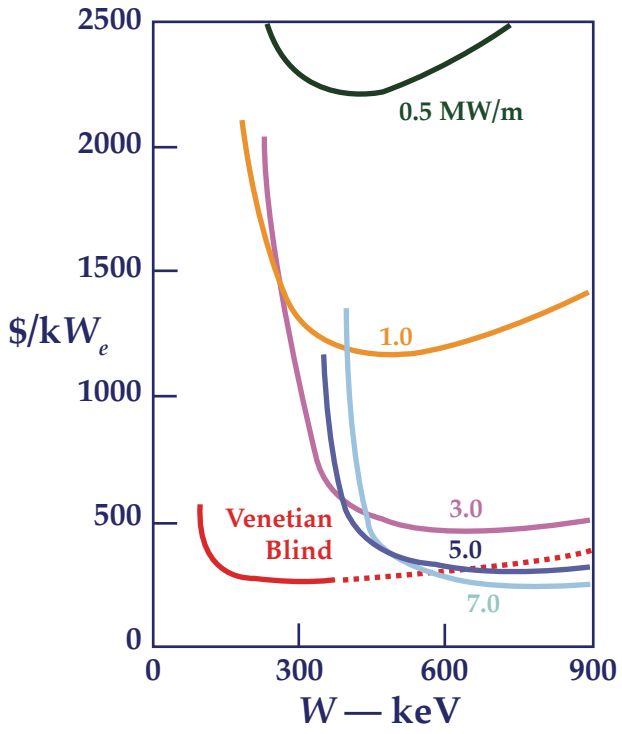

Figure 16 — Cost estimate for the direct converter per net kW out of the reactor as a function of mean ion energy.

Figure 16 shows that the cost of the direct converter must be reduced substantially to be economically competitive. Costs might be reduced by:

- Stacking several collectors within one vacuum chamber. Since most of the cost is in the vacuum chamber, it would appear that the cost can be decreased linearly with the number of stacked collectors per chamber.
- Providing more focusing with magnetic fields in addition to the electrostatic fields presently used. This would be to handle more power.
- Increasing the circumference-to-area over that of a circle by going to elliptical shapes.

Finally, we should note that radically different ideas not just modifications to the periodic focusing idea — may be required to reduce costs. The Venetian Blind concept is such idea; the one-stage version is so simple and inexpensive that there is justification for working on it to improve its efficiency.

Future Plans

Our immediate plans involve verifying the calculated efficiencies with our new experimental facility. We are going to work at low power levels at first and then increase the density to measure effects of space charge. We also plan to investigate, by both experiment and calculation, other schemes for direct conversion — especially those schemes that can increase the power density limits.

Publishing History

Received January 3, 1977. First published December 1977.

Reformatted and color illustrations in March 2009 by Mark Duncan.

References

[1] Richard F. Post; in Proceedings British Nuclear Energy Society Conference on Nuclear Fusion Reactors, Culham Laboratory, Culham, England pp. 88-111(1969).

[2] Ralph W. Moir, William L. Barr, Robert P. Freis, and Richard F. Post; in Proceedings Conference Plasma Physics and Controlled Nuclear Fusion Research, International Atomic Energy Fusion, Vienna, pp. 315-328, (1971).

[3] Barry C. Howard, William L. Barr, Ralph W. Moir; DART: A Simulation Code for a Direct Energy Converter for Fusion Reactors, Lawrence Livermore Laboratory Report UCRL-51557 (1974).

[4] Bobby H. Smith, Richard H. Burleigh, Warren L. Dexter, and Lewis L. Reginato; in Proceedings Texas Symposium on the Technology of Controlled Thermonuclear Fusion Experiments and the Engineering Aspects of Fusion Reactors, Austin, Texas (1972).

[5] The energy distribution of particles leaking to a mirror machine was calculated by Artcher H. Futch and refined by Lawrence S. Hall using the Fokker-Planck computer code of Reference 17.

[6] F. B. Marcus and C. J. H. Watson; in Sixth European Conference Controlled Fusion and Plasma Physics, Moscow, USSR, (July-August 1973).

[7] Richard W. Werner, Gustav A. Carlson, Jack Hovingh, Joseph D. Lee, M. A. Peterson, in Proceedings Texas Symposium on the Technology of Controlled Thermonuclear Fusion Experiments and the. Engineering Aspects of Fusion Reactors, Austin, Texas, (1972).

[8] U. A. Arifov, R. R. Rakhimov, M. Adbullaeva, and S. Gaipov, Engineering Transactions: Bulletin Aoad. Science USSR, Physics Ser. (USA) 26, No. 11 1427-31 (1963).

[9] M. Kaminsky, Atomic and Ionic Impact Phenomena on Metal Surfaces Academic Press, Inc. New York; pp. 315-319 (1965).

[10] L. N. Large; Proceedings Physics Society, 81,1101 (1973).

[11] George H. Miley and Ralph W. Moir; in Proceedings Fifth Symposium Engineering Problems of Fusion Research IEEE Trans. Nuclear Science, Princeton, New Jersey, (1973).

[12] William L. Barr, Losses Due to Ionization and Charge Exchange in the Channel of the Direct Converter, Lawrence Livermore Laboratory, Report UCID-16112. See also Reference 7, p. 76 (9172).

[13] Gustav A. Carlson; Selective Leakage of Charged Particles in Mirror Machines, Lawrence Livermore Laboratory, Report UCRL 51434 (1973).

[14] Ralph W. Moir, William L. Barr, and Richard F. Post; Physics Fluids, 14, 2531 (1971).

[15] See Reference 7, p. 55.

[16] William L. Barr, Richard J. Burleigh, Warren L. Dexter, Ralph W. Moir, and Richard R. Smith; A Preliminary Engineering Design of a Venetian Blind Direct Energy Converter for Fusion Reactors, Lawrence Livermore Laboratory, Report UCRL 74636 (1973).

[17] Artcher H. Futch Jr.; J. P. Holdren, John Kileen, and A. A. Mirin; Plasma Physics, 14, 211 (1972).

[18] J. Hovinghand; Ralph W. Moir; Efficiency of Injection of Neutral Beams into Thermonuclear Reactors, Lawrence Livermore Laboratory, Report UCRL-74883 (1973).

[19] Ralph W. Moir and J. D. Lee; Criteria for Design of a Adiabatic Expander for a Direct Energy Converter, Lawrence Livermore Laboratory, Report UCRL 51351 (1973).

[20] Blake Myers; In Fifth Intersociety Energy Conversion Engineering Conference Energy 70, Las Vegas, Nevada (1970).

[21] Blake Myers; Lawrence Livermore Laboratory, private communication (1974).